Growing and stability of gold nanoparticles and their functionalization by cysteine

Andrea Majzik[1], Rita Patakfalvi[2], Viktória Hornok[1] and Imre Dékány[1,2]

[1] Supramolecular and Nanostructured Materials Research Group of the Hungarian Academy of Sciences, Department of Colloid Chemistry University of Szeged, 6720 Szeged Aradi vt. 1
[2] Department of Colloid Chemistry, University of Szeged, H-6720 Szeged, Aradi Vt. 1. Hungary
Corresponding author: Imre Dékány,
e-mail address: i.dekany@chem.u-szeged.hu

Abstract

Gold nanoparticles in aqueous dispersion were prepared using the trisodium citrate reduction method to control the size of particles by changing the concentration of $HAuCl_4$. The average particle size measured by DLS is higher than that obtained by TEM at a zeta potential of -40 mV. When trisodium citrate concentration is kept constant, the particle size increases with gold concentration. The kinetics of growth was studied and apparent kinetic rate constants were determined at various gold/citrate ratios. Gold nanoparticles were attached to silanized glass surfaces; Au rods were grown (ca. 200 nm) by adding more precursors and the rods' growth rate was monitored by UV-Vis spectroscopy as well as by AFM. Surface functionalization of gold surface was influenced by cysteine. The surface modification by cysteine at pH=6.0 results in aggregation and the red shift of absorption maximum is nearly 200 nm. When glutathione molecules are bound onto the cysteine-linked Au rods on the glass surface, the spectral shift reaches only an amount of 5-10 nm, because the surface attachment hinders the tendency to aggregate.

Keywords: gold, sodium-citrate, nanorods, cysteine, kinetics of growing, aggregation, functionalization, glutathione

1 Introduction

Research into the preparation and biological applicability of noble metal nanoparticles with nearly monodisperse size distribution and arbitrarily variable size and geometry has attracted considerable interest [1]. The first reproducible method was presented by Turkevich, who synthesized Au nanoparticles with a diameter of 20 nm via reduction of $HAuCl_4$ by trisodium citrate [2]. In general, the geometry of the particles depends on the quality of the precursor, whereas the particle size depends on the precursor/reducing agent ratio [3]. Y.Q. He et al. prepared gold sols with different particle sizes (12-41 nm) that depended on the amount of trisodium-citrate [4]. The colour of the sols ranged from reddish orange (520 nm) to reddish purple (530 nm) depending on particle size. Saraiva and Oliveira [5] called attention to the fact that the preparation of $HAuCl_4$ using citrate is influenced by a number of factors including temperature and reactant concentrations. The authors studied the nascent particle size as a function of the rate of trisodium citrate addition, which is another important factor in the process. Y. Luo employed natural sunlight to synthesize size-controlled gold nanoparticles stabilized by polyethylenimine; particles of ca. 25 nm diameter were obtained [6]. In another study published in 2007, Y. Lou reported a one-step synthesis method yielding particles with various sizes: this procedure uses 3-thiophene-malonic acid as reducing and protective agent [7, 8]. PDDA [poly(diallyldimethylammonium chloride)] has also proved to be suitable as a reducing and stabilizing agent for the preparation of particles measuring ~12 nm [9]; gold nanoparticles may also be synthesized and stabilized using ascorbic acid [10].

The work of Liz-Marzán et al. is of fundamental importance in the preparation of nanoparticles of various shapes (spherical and anisometric, rod-like and prism-shaped) [11- 13]. The resonance wavelength of anisometric particles such as nanorods depends on the orientation of the electric field. [14].

The interaction of gold and silver nanoparticles with biomolecules has been studied intensively [15, 16]. Since metal nanoparticles surface plasmon oscillations in the visible wavelength range, their optical properties [17] attract intense scientific and technological interest. Zhong et al. showed that gold nanoparticles reduced and stabilized by citrate have a negative surface charge and preferentially bind to thiol, amine, cyanide or diphenylphosphine functional groups [18]. Binding via α-amino groups is preferential at low pH and is suppressed at neutral and high pH, due to electrostatic repulsion between the surface of gold and the charged carboxyl groups.

In the work presented here, reproducibly size-controlled gold nanoparticles reduced and stabilized by citrate were synthesized in aqueous dispersions. The kinetics of the gold nanoparticles formation was also studied. Gold nanorods were grown on functionalized glass surface and the rate

constants were determined. The surface of Au nanoparticles was modified by amino acids (cysteine and glutathione) and the effect of pH and increasing cysteine concentrations on the dispersions was investigated. The surface-growth of Au nanorods, the effect of the chemisorptions of cysteine and glutathione were characterized by the shift of plasmon resonance maxima in the absorption spectra.

2 Materials and methods

Preparation and kinetic control of gold nanoparticle growth

Au nanoparticles were prepared by Turkevich method [2]. For the preparation of Au nanoparticles: $HAuCl_4{}^*3H_2O$ (Sigma-Aldrich), tri-Na-citrate (Reanal) in MQ (Milli-Q) water were used. The $HAuCl_4$ was dissolved and was heated until boiling and while stirring vigorously, the sodium citrate solution was added and kept stirring for the next 30 minutes. The colour of the solution would change until setting on wine-red. The sodium citrate acts as a reducing and stabilizing agent. The formation of Au nanoparticles was followed by Ocean Optics Typ Chem 2000-UV-VIS diode array spectrophotometer (Florida, USA) at wavelength λ=200-800 nm. During preparation, the absorbance spectrum of the 3 cm^3 sample was recorded from time to time and the mixture was stirred with a micro-magnetic stirrer at 25±0.1°C. Following the changes in absorbance spectrum added cysteine (Reanal) to the nanosols was recorded every minute within 30 min, starting at the moment of the addition of amino-acid.

Preparation of gold nanorods

Materials used for the preparation of Au nanorods were: 3-mercaptopropyl-trimethoxysilane (MPTMS, Aldrich), $HAuCl_4{}^*3H_2O$ (Sigma-Aldrich), cetyl-trimethyl-ammonium-bromide (CTABr, Reanal), L+ ascorbic acid (Reanal) and MQ water.

The glass substrates were treated with MPTMS and then with citrate stabilized gold nanoparticle seeds at different concentrations and growth solution which containing cetyl-trimethyl-ammonium-bromide, ascorbic acid and gold ions [19, 20]. Kinetics of the growth of nanorods from containing 0.1-1 mM $HAuCl_4$ solutions was recorded by diode array spectrophotometer at wavelengths λ=200-800 nm. TEM images were performed in a Philips CM-10 transmission electron microscope at 100 kV. The microscope was equipped with a Megaview II digital camera. TEM grids were prepared on a Formwar foil covered copper grid. The size distribution was determined by using UTHSCSA Image Tool 2.00 software.

The growth of Au nanorods was also monitored by a Nanoscope III Multimode AFM (Digital Instruments, USA) using a piezo scanner with scanning capability of 12.5 μm in x and y direction and 3 μm in z direction, tapping-type tip of silicon (Veeco Nanoprobe Tips RTESP model, 125 μm length, 300 kHz). Particle size and size distribution were measured by dynamic light scattering (DLS) apparatus and the Zeta potential data were obtained by a Zetasizer Nano ZS ZEN 4003 (Malvern Instrument, UK). The measurements were recorded at 25±0.1°C. Since the zeta-potential measurements were performed in an aqueous solution, the Smoluchowski approximation was used to calculate the zeta-potentials from the measured electrophoretic mobility.

3 Results and discussion

A method was developed for the controlled synthesis of gold nanoparticles in aqueous medium by reduction using trisodium citrate dihydrate at 25°C. Size and size distribution of the particles formed and the colloid stability of the obtained gold dispersions were studied. The most commonly used preparative method is reduction by trisodium citrate. We studied the effect of variations (i) in the gold:citrate ratio in the composition range of 1:1 - 1:20 (where $c_{Au}{}^{3+}$=0.2 mM and $c_{citrate}$=0.2-4 mM) (Fig. 1a,b) and (ii) in the initial gold concentration (in the range of 0-1 mM, $c_{citrate}$=2 mM) on the size of nascent particles (Fig. 2a). The absorbance spectra of the Au nanoparticles formed was determined after a 24-hour reaction time following preparation (Fig. 1a). It is clearly shown in Fig. 1a that the plasmon resonance maximum of gold particles varies within the wavelength range of 533-544 nm, depending on citrate concentration. Maximum absorbance values are seen to increase when the amount of added citrate is increased from a ratio of 1:1 to 1:3 and to decrease within the ratio range of 1:3 - 1:20, which may be due to the formation of particles of different sizes depending

Figure 1a

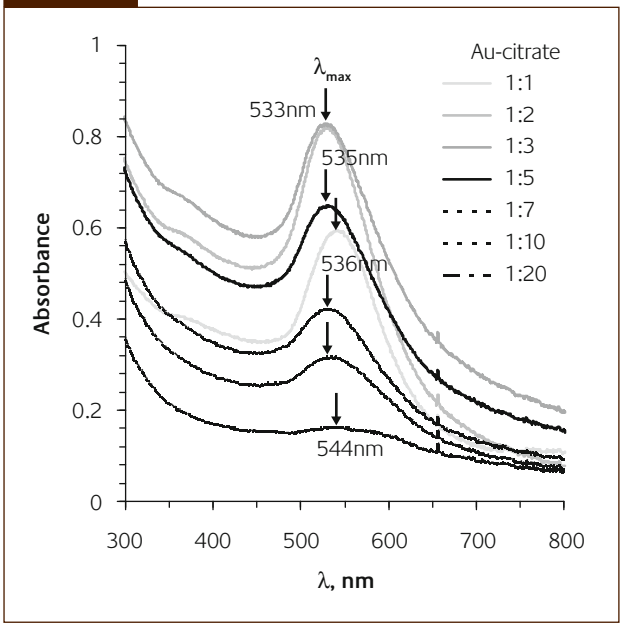

Absorption spectra of gold nanoparticles at ratio of gold/citrate 1:1-1:20 ($c_{citrate}$=0.2-4mM and $c_{Au}{}^{3+}$ = 0.2 mM) after 24 hours reduction time

Figure 1b

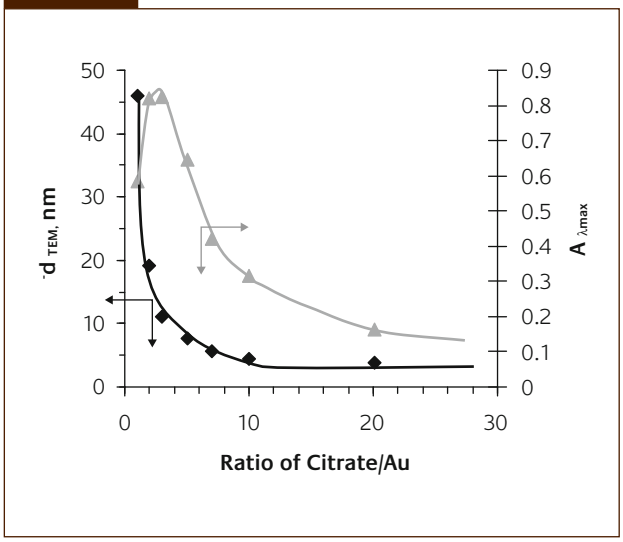

Relation between the maximum absorption values and the diameter at increasing citrate/gold ratio (c_{Au}^{3+} =0.2 mM) after 24 hours reduction time

Figure 2a

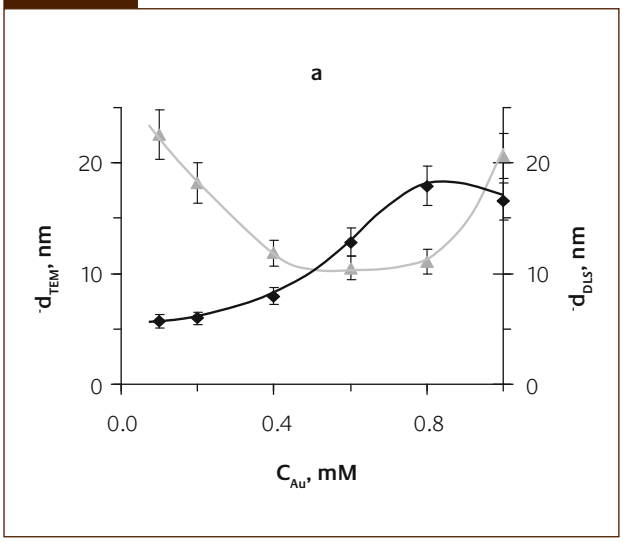

Relation between the particle size measured by TEM and DLS and the original gold concentration (c_{Au}^{3+} = 0.1-1 mM and $c_{citrate}$=2 mM)

Figure 2b

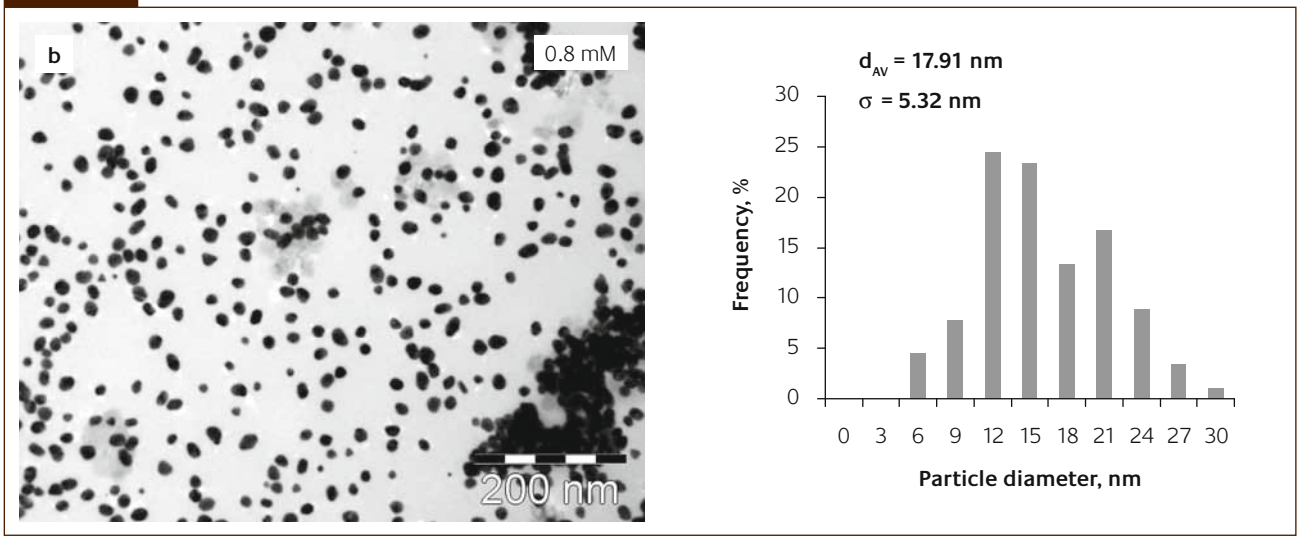

TEM image of c_{Au}= 0.8 mM (~18 nm) nanodispersion

on citrate concentration. The more citrate is present, the smaller are the nascent particles owing to the stabilizing effect of citrate. Relatively large gold nanoparticles are characterized by narrow, well-defined peaks, whereas smaller particles by broader, less sharp maxima (Fig. 1a) [21]. To determine the size of the Au nanoparticles formed in the various gold dispersions, samples were prepared on copper grids 24 hours post-reduction. Particle diameters determined in TEM images (Fig. 1b) decrease exponentially with increasing amount of citrate and absorbance maxima change in a nearly parallel fashion, i.e. an initial maximum is followed by nearly exponential decrease. At Au:citrate=1:1 (c_{Au}=$c_{citrate}$ =0.2 mM) the size of the particles formed was ~46 nm, whereas at Au:citrate ratios of 1:10 (c_{Au}=0.2 mM, $c_{citrate}$ =2 mM) and 1:20 (c_{Au} =0.2 mM, $c_{citrate}$ =4 mM) the particle diameter stagnated at ~5 nm, due to the stabilizing effect of large excess of citrate present. These values are in good agreement with the experimental results reported in the literature [4].

According to Fig. 2a, increasing the initial concentration of $HAuCl_4$ 0.1-1 mM results in a continuous increase in particle size at a constant citrate ion concentration of 2 mM. As precursor concentration is increased, increasingly larger particles (5-18 nm) are obtained by the evidence of the particle size distribution curves based on TEM images. Particle sizes determined by DLS (10-22 nm) (Fig. 2a), however, do not match those determined on the basis of TEM images (5-18 nm). The TEM image and the size distribution of gold

Figure 2c

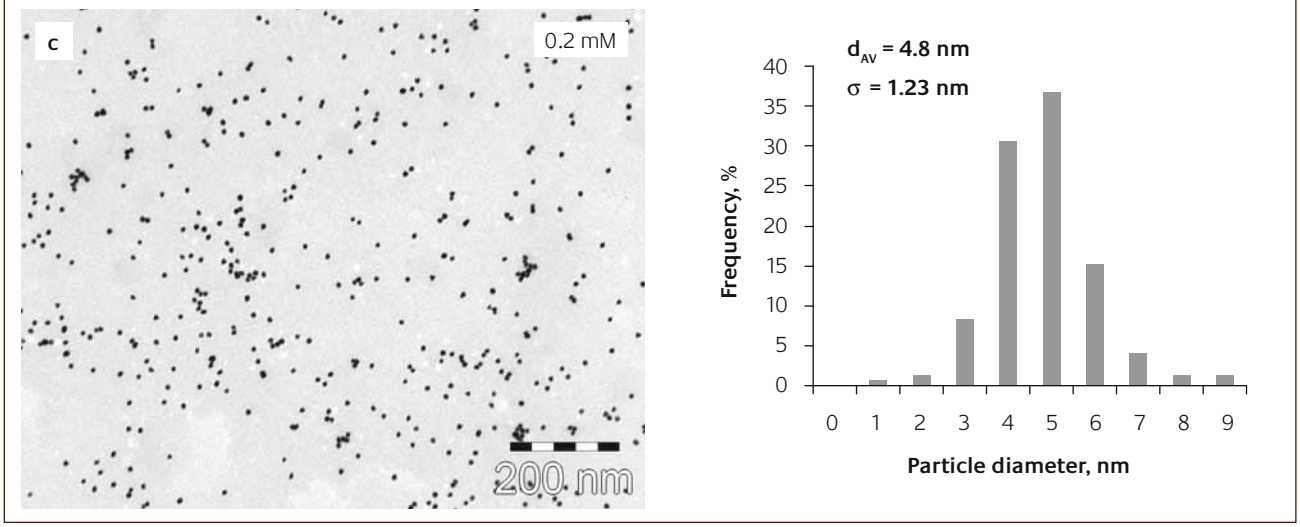

TEM image of c_{Au} = 0.2 mM (~5 nm) nanodispersion

Table 1

Particle diameters (nm) determined by TEM and by DLS as a function of initial gold concentration (mg/ml and mM) and the corresponding aggregation ratios (constant $c_{Na\text{-}citrate}$ = 2 mM)

c_{Au}, mg/ml	c_{Au}, mM	d_{DLS}, nm	d_{TEM}, nm	Zeta-potential, mV	aggregation ratio (d_{DLS}/ d_{TEM})
0.034	0.1	22.57±4.00	5.69±2.41	-23.0±1.15	3.97
0.068	0.2	18.21±4.30	5.95±2.05	-29.4±1.47	3.06
0.136	0.4	11.85±3.92	7.97±1.94	-39.7±1.56	1.49
0.204	0.6	10.50±1.83	12.83±4.18	-41.8±2.09	0.82
0.272	0.8	11.09±1.40	17.91±5.32	-40.3±2.01	0.62
0.340	1	20.62±1.52	16.52±5.00	-41.8±2.06	1.25

nanoparticles formed in the solution containing 0.8 mM $HAuCl_4$ are shown in Fig. 2b. The average diameter of the particles is ~18 nm, whereas in the samples containing 0.2 mM $HAuCl_4$ particles measuring ~5 nm were formed (Fig. 2c). Size distribution is more homogeneous in dispersions containing smaller particles than in those of larger particles. The higher extent of homogeneity is due to the presence of larger amount of citrate ions. The application of lower citrate/Au ratio (1:5) leads to a decrease in the stability of Au dispersions, resulting in the aggregation of gold nanoparticles.

Particle size determined by DLS method provides information on the size of aggregates rather than on the diameter of individual nanoparticles. If the particle size obtained by DLS measurement is divided by values of TEM average particle size the aggregation ratio characteristic of the adhesion between the gold nanoparticles is yielded (Table 1).

As shown in Table 1 at relatively high gold concentrations (0.6-1 mM) aggregation ratios are close to 1, whereas at lower gold concentrations the particles obtained are increasingly smaller and inhibit aggregation. This is due to the presence of identical concentrations of citrate ions (2 mM) in dispersions containing smaller and larger particles. In dispersions with smaller particles, the number of citrate ions per particle is lower; consequently the stabilization by citrate is less extensive, resulting in a stronger tendency to aggregate.

Zeta potentials of gold dispersions containing 2 mM of citrate and 0.1-1 mM of gold are shown in Fig. 3. The values of zeta potential vary in the range of -25 to -42 mV within the series. Decreasing the concentration of the precursor, i.e. increasing the citrate/gold ratio leads at citrate/gold ratios higher than ~3, to a significant increase in zeta potential. When precursor concentration is increased (the citrate/gold ratio is decreased), the number of $AuCl_4^-$ ions in the dispersion increases due to dissociation, and acting as stabilizer these enfold the reduced gold nanoparticles. The higher the

Figure 3

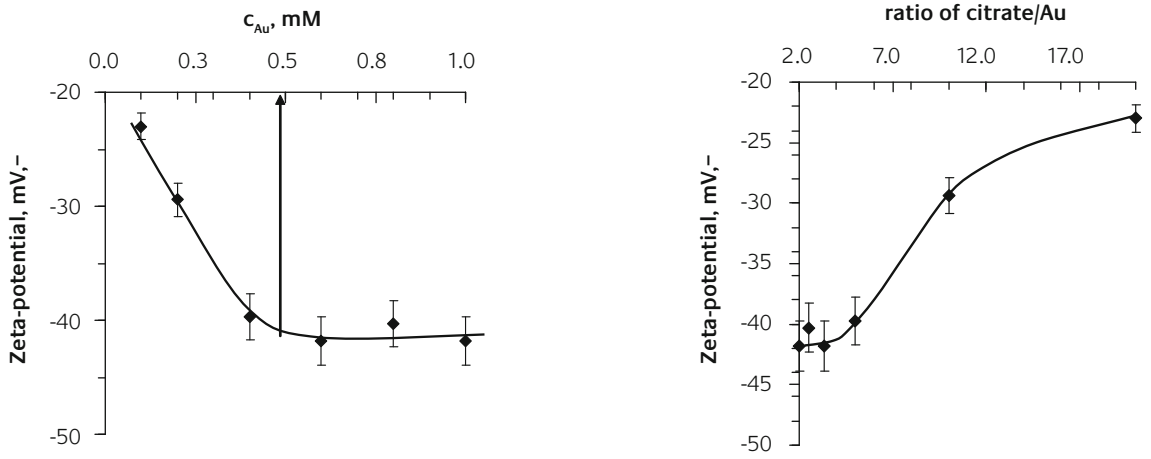

The change of zeta-potential (mV) increasing the precursor concentration (mM) ($c_{citrate}$=2 mM, c_{Au}=0.1-1mM)

Figure 4

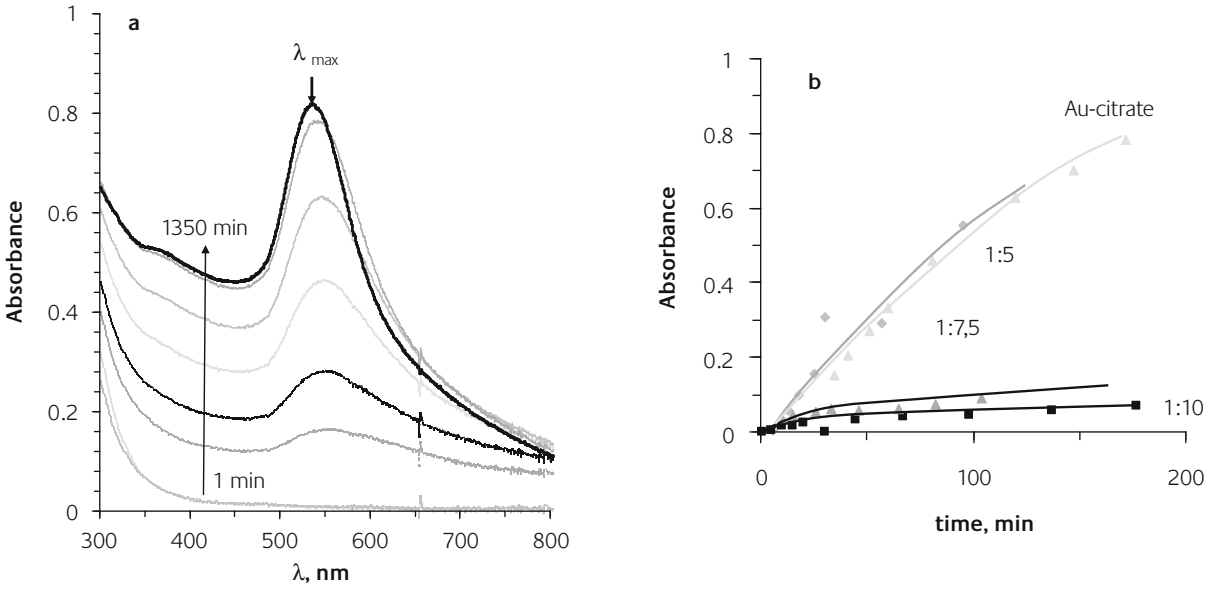

Absorption spectra of gold nanoparticles formation in the Au/citrate 1:1 gold nanodispersion (a) and the kinetics of gold nanoparticles formation in Au/citrate 1:1, 1:5, 1:7.5 and 1:10 systems (b)

concentration of $AuCl_4^-$ ions in the dispersions, the more negative zeta potential values are measured, until the value of ca. -40 mV is reached and zeta potential does not decrease any further. Similar results were obtained by Brewer et al. [22] for values of zeta potential in gold dispersions reduced and stabilized by citrate, at pH ~5-6.

The kinetic of nanoparticle growth

The kinetics of nanoparticle formation was studied at Au/citrate ratios of 1:1, 1:5, 1:7.5 and 1:10 (Fig. 4). The spectra in the left panel of the Figure demonstrate the formation of gold particles of the sol containing 2 μmol of $HAuCl_4$ and 2 μmol of trisodium citrate. The absorbance resonance maximum appeared after about 20 minutes. Gradual sharpening/narrowing of the peak and gradual increases in absorbance values reach their maxima in ~24 hours, at this time the reduction process is complete. Fig. 4 clearly demonstrates that as citrate concentration is increased, gold nanoparticles take increasingly longer to form, which can be attributed to the stabilizing effect of citrate. The rate of gold particle formation (Table 2) is characterized by the slope fitted to the straight, initial sections of the curves, corresponding to the apparent equilibrium constants (k*).

Table 2

Values of the apparent equilibrium constants (k) at various Au/citrate ratios*

Au/citrate ratio	K*, 1/min
1:1	$8.4^{*}\ 10^{-3}$
1:5	$6.0^{*}\ 10^{-3}$
1:7.5	$1.8^{*}\ 10^{-3}$
1:10	$1.4^{*}\ 10^{-3}$

Kinetics of gold nanorod growth

Gold nanosols reduced and stabilized by citrate were also used for growing gold nanorods, and to determine the kinetics of growth and the detectability of functionalized surfaces were investigated by recording UV-Vis spectra. Nanorods were grown in the following way. Previously synthesized gold nanoparticles were spread on the surface of microscope slides that had been thoroughly cleaned in chromosulfuric acid and functionalized by MPTMS (Fig. 5). The silanized glass plates were left to stand in the gold sol for 25 min. The surface-modified glass plates carrying the gold

Figure 5

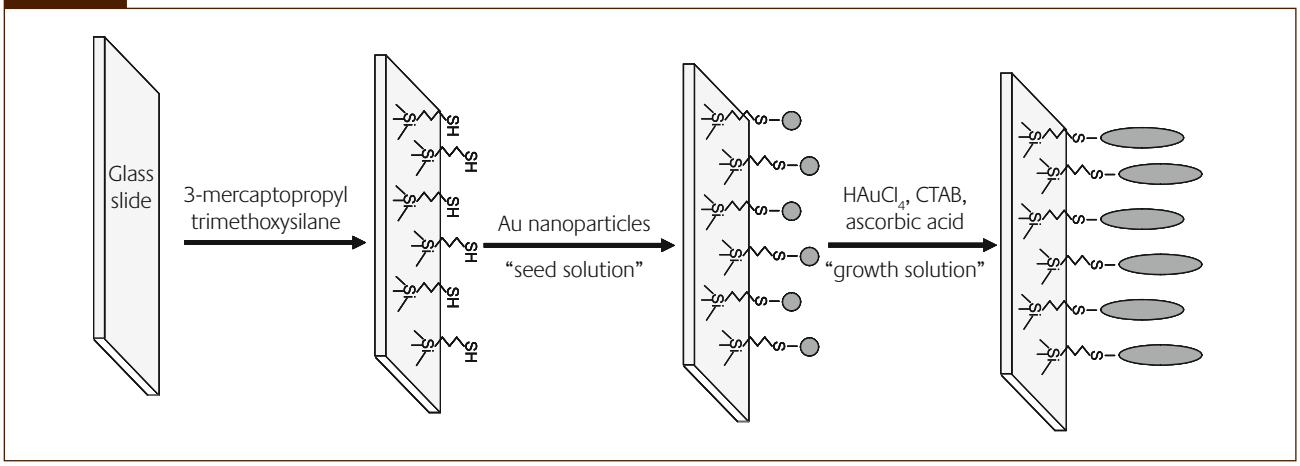

The scheme of gold nanorods formation onto modified glass surface

Figure 6

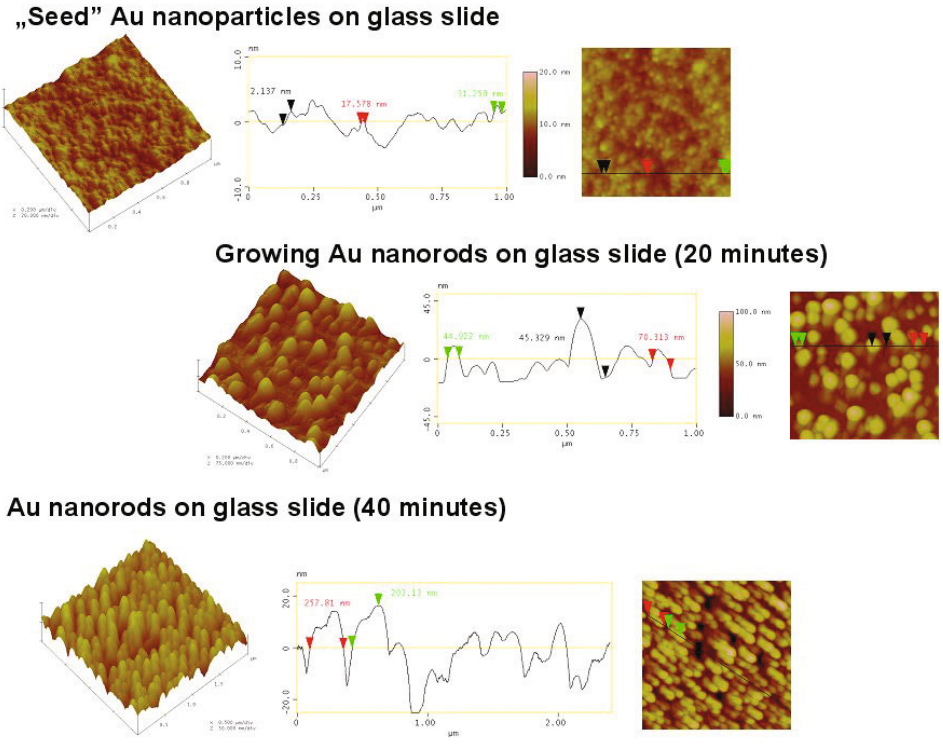

Growing of the gold nanorods on modified glass surface monitored by AFM. The growing solution contained 1 mM $HAuCl_4$ and $5x10^{-4}$ M ascorbic acid as reducing agent

Figure 7

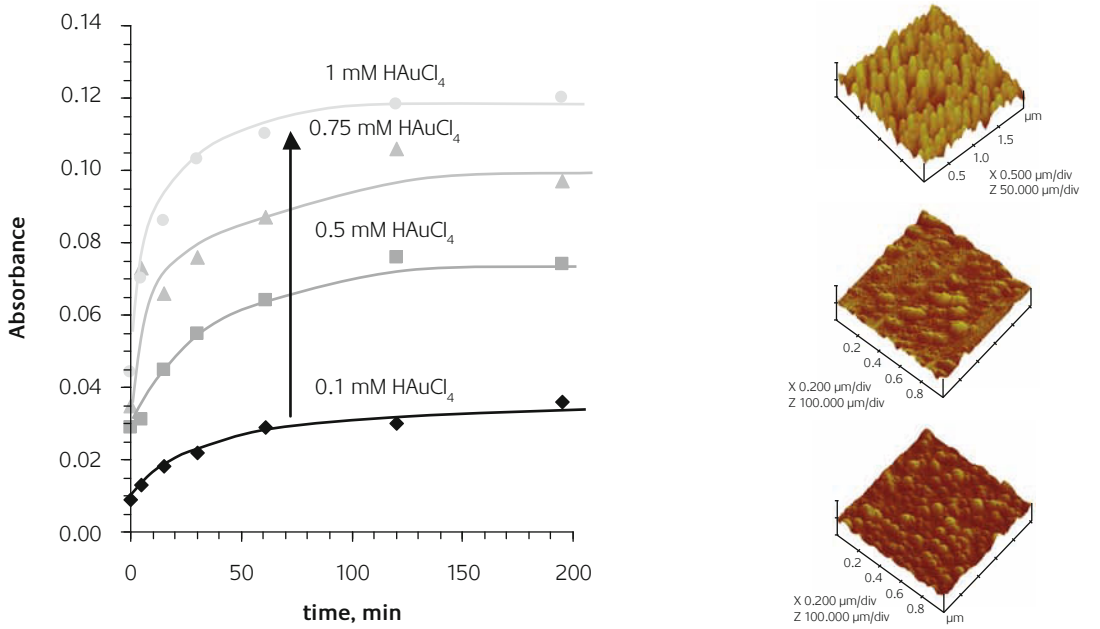

AFM images and kinetics of the gold nanorods growing from containing 0.1-1 mM $HAuCl_4$ growing solutions which contained $5x10^{-4}$ M ascorbic acid as reducing agent

Figure 8

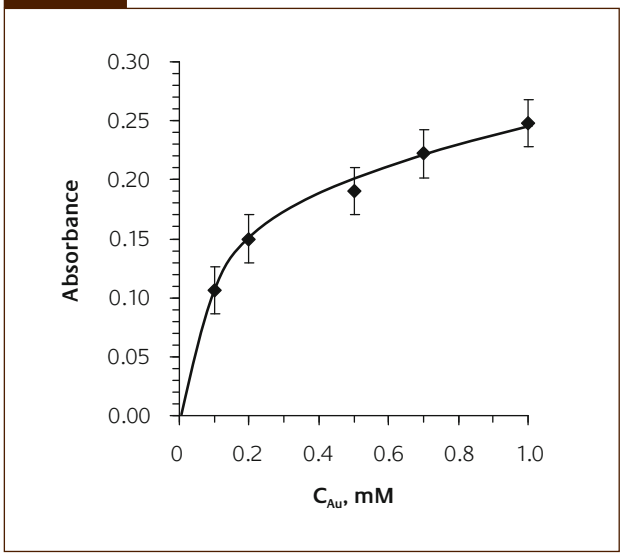

Maximum absorbance values of the gold nanorods from 0.1-1 mM $HAuCl_4$ containing growing solutions at λ=530 nm

nanoparticles were then immersed into the "nanorod growth solution" consisting of 0.1 M CTAB, 100 µl of 0.05 M $HAuCl_4$ and 0.05 ml of 0.1 M ascorbic acid.

The nanorod growth process was studied by AFM (Fig. 6). In the course of growth, the difference between rods grown for 0, 20 and 40 min is well discernible in the diameter analysis plot based on the AFM images. The diameter of rods grown for 20 min were ~45 nm, whereas the height of rods grown for 40 min was ~200 nm and their diameter was ~120 nm. Following 40-45 min growth the height of rods did not change any more.

In the course of our kinetic studies on the growth of gold nanorods on microscope slides previously treated in an identical fashion (silanized and subsequently immersed in a sol of identical concentration) were immersed into growth solutions containing $HAuCl_4$ in various concentrations (0.1-1 mM). Our experience showed that depending on the concentration of the growth solution, different amounts of gold particles adhere to the surface-modified microscope slide. The kinetics of nanorod growth are presented in Fig. 7. In the presence of higher amount of $HAuCl_4$, increasing number of particles can attach to the surface, resulting in the formation of thicker layer, as evinced by the increasing absorbance values. The nanorod growing process in 0.1-1 mM $HAuCl_4$ is shown in Fig. 8. As initial gold concentration is increased the saturation curves representing higher concentrations are positioned one above the other and reach increasingly higher maximal absorbance.

Effects of thiol groups in the bulk phase and on the silanized glass surface covered with gold

The surface of the particles synthetized was modified in chemisorption processes by the thiol-containing compound cysteine. Functionalization of the gold surface by cysteine was monitored and the effect of pH and increasing cysteine concentrations on the resonance values of the absorbance spectra was studied (Fig. 9). Gold nanoparticles are located apart each other according to TEM images (Fig. 2.c) because they are stabilized by citrate. The sodium citrate acts as a

Figure 9

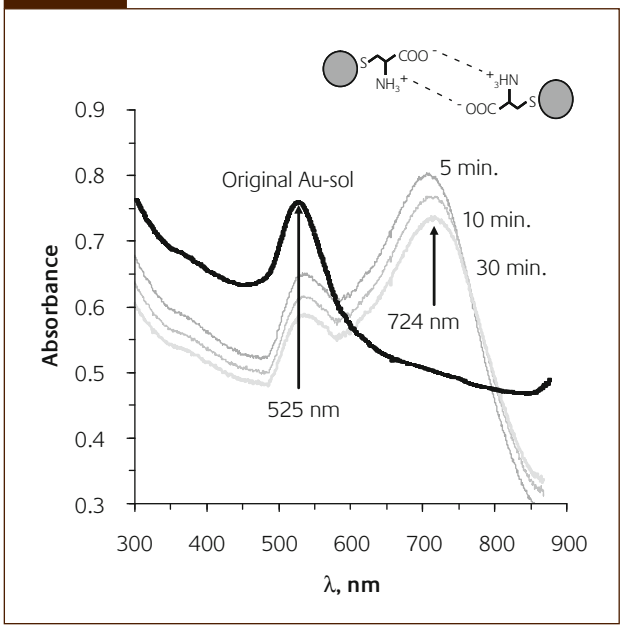

Absorption spectra of citrate stabilized gold nanodispersion (0.3 mM) and the effect of added cysteine (0.4 mM). (Δ λ= 199 nm)

Figure 10

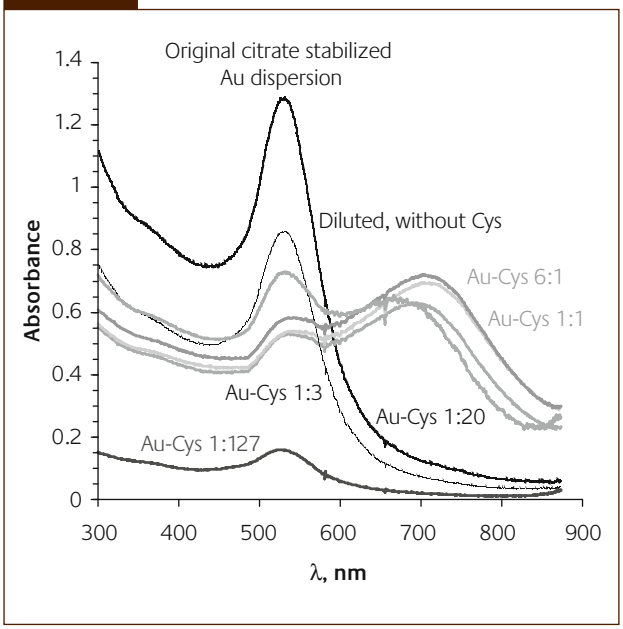

Absorption spectra of Au nanodispersions at various cysteine concentration at pH~6. (Δ λ = 155-199 nm)

Figure 11

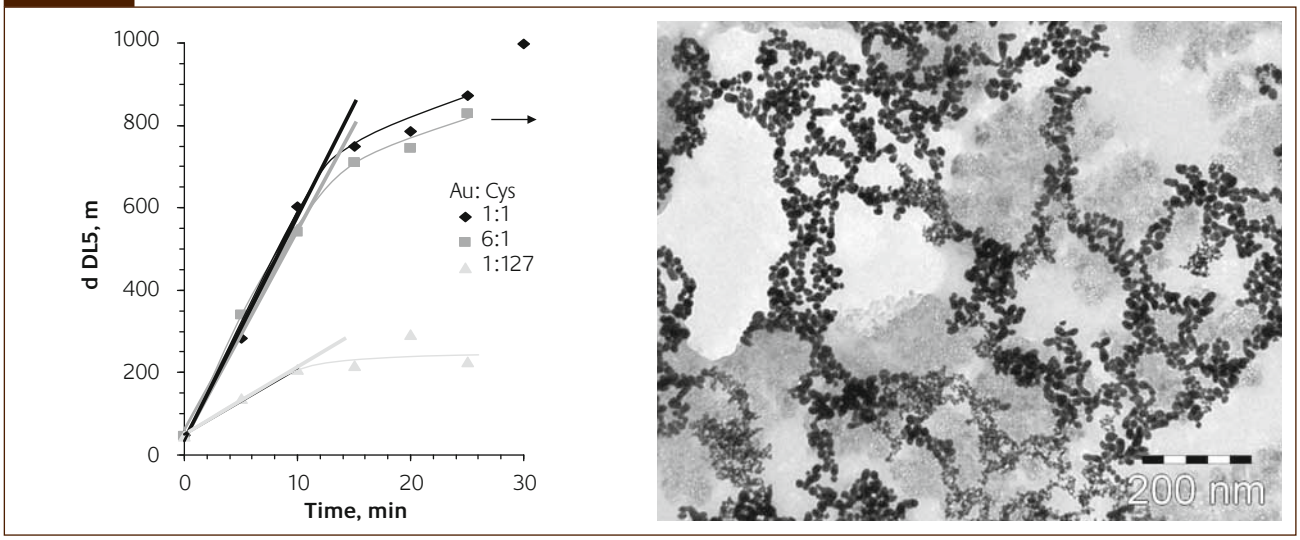

Change of particle diameter measured by dynamic light scattering for gold nanodispersions at Au:Cys 1:1, 6:1 and 1:127 ratio and TEM image on particle network at Au:Cys 6:1 ratio

reducing agent, and the citrate anions are adsorbed onto the gold nanoparticles and establish the surface diffuse layer that repels the particles from one another and prevents them from aggregation. In the presence of cysteine under acidic condition functional groups of cysteine are protonated (the thiol groups bind to gold surface), so the cysteine molecules constitute bridge among gold nanoparticles, thus large aggregates form, which deposit in time.

As a result of the addition of cysteine, a new peak appears in the UV-Vis spectra at about 730 nm, which may be characteristic of gold particles aggregating as a consequence of the electrostatic attraction between positively charged NH_4^+ and negatively charged COO^- groups present at pH<6. This peak does not appear at pH~10, since at this pH the repulsion of negative charges keeps the gold nanoparticles apart. Following the addition of cysteine two new peaks are observed in the spectrum: the first peak located near the resonance peak for single particles is attributed to quadrupole plasmon excitation in coupled spheres, whereas the second peak at a longer wavelength is attributed to the dipole plasmon resonance of gold nanoparticles [23].

If the concentration of cysteine is increased to that of gold, the peak appearing at about 730 nm shifts towards lower wavelengths, and at sufficiently high cysteine concentrations (Au:Cys =1:127) the second peak does not appear at all, which may be due to the relatively large distance

Figure 12

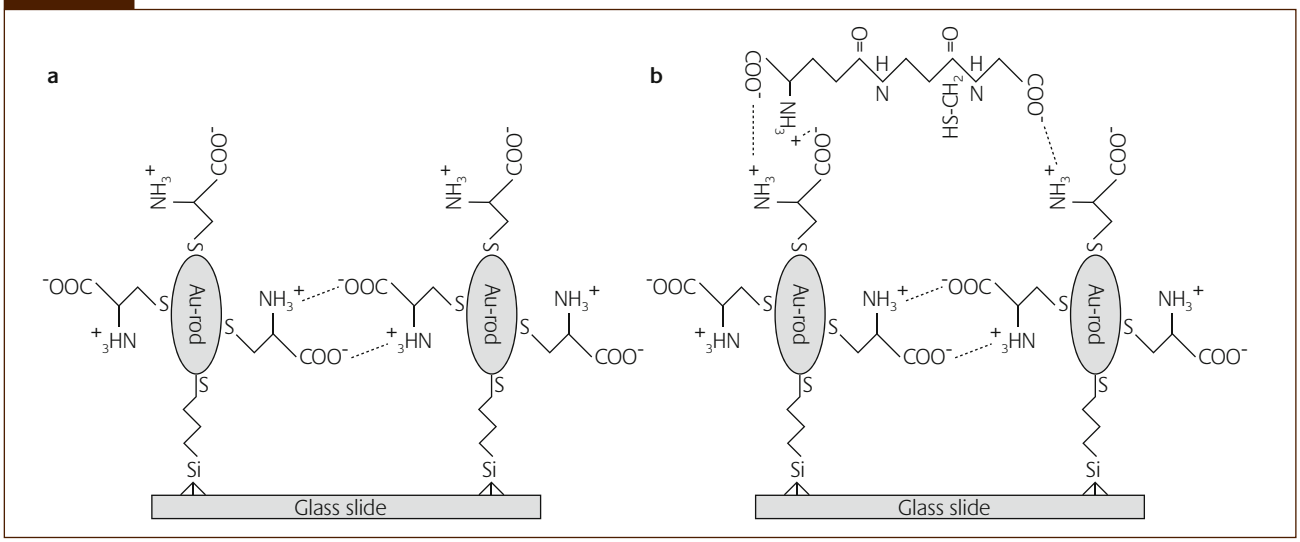

Schematic picture of gold nanorods with cysteine, fixed to solid phase (a) and attach of glutathione (b) on the gold nanorods

Figure 13

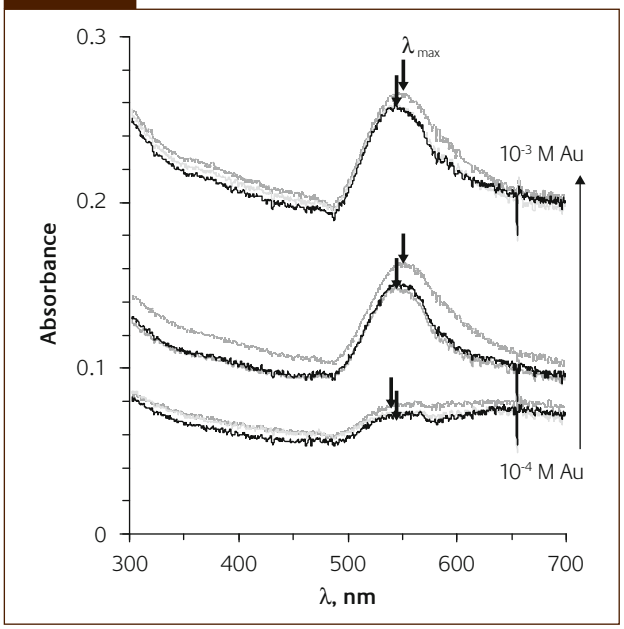

Absorption spectra of nanorods which was growing from 10^{-4} – 10^{-3}M growing solution (black curve), with cysteine (10^{-3}M, light grey curve) and with glutathione (10^{-3}M, deep gray curve) at pH ~4.5

separating the individual gold nanoparticles (Fig. 10). When cysteine was the only reducing agent present during gold particle synthesis, the plasmon resonance maximum of the particles formed is shifted towards the infrared region by about 30 nm and the new peak observed at about 700 nm in this case fails to appear [24].

The formation of aggregates induced by the addition of cysteine can also be conveniently followed by dynamic light scattering measurements (Fig. 11), whose results are in good agreement with the formation of peaks characteristic of aggregation in the spectra. According to DLS, at Au:Cys ratios of 1:1 and 6:1 the approximate size of the aggregates is ~800-900 nm, whereas at a ratio of 1:127 it is measured to ~200 nm (Table 3). The slopes of lines fit to the initial regions of the curves provide information on the rate of aggregate formation. The Figure clearly shows that upon increasing cysteine concentration, aggregate formation becomes slower and aggregate size falls below that observed in the presence of lower concentrations of cysteine. The rate of aggregate growth in the sol with 1:1 composition is 55.5 nm/s; in the case of the dispersion containing an excess of gold this rate is 49.5 nm/s and it is even lower, 16.1 nm/s in the dispersion containing a large excess of cysteine. These values confirm the location of the new absorption peaks appearing at about 700-720 nm (Fig. 10) and indicating the presence of newly formed aggregates. Fig. 11 shows the time dependence of particle diameter values calculated from DLS measurements.

The 3-D particle lattice (aggregate) forming in the presence of cysteine, confirming the size of ~800-900 nm determined by DLS is shown in Fig. 11 (to be compared with Fig. 2, the TEM image of gold particles stabilized with citrate). Formation of the 3-D particle lattice is due to electrostatic attraction [25]. At the pH corresponding to the isoelectric point, the protonated carboxyl group of cysteine molecule covalently bound to the negatively charged gold particle binds to the protonated amino group of the neighbouring molecule, forming a bridge to link individual gold particles together. The above shown aggregate is the result of the binding of further particles. Horovitz et al. (2007) bound protein to gold particles. Their TEM images taken at various magnifications, however, do not provide convincing proof for the way the aggregates form. Due to the presence of thiol group, addition of the tripeptide glutathione to aqueous gold dispersions brings about changes in the UV-Vis spectrum similar to those caused by cysteine. In time the new peak appears at ~660 nm, at the appropriate pH.

When cysteine is linked to nanorods, followed by glutathione (Fig. 13), monitoring changes by spectrophotometry becomes more difficult. Since gold nanoparticles are fixed on the surface (Fig. 12), the spectra of rods synthetized from growth solutions with different gold concentrations exhibit only minor shifts even after the addition of cysteine followed by glutathione. The maxima of the peaks shift with increasing gold precursor concentration towards the red wavelength range (Fig. 13). The absorbance maximum decreases and blue shift (2-3 nm) can be detected by the effect of cysteine; after the addition of glutathione, the absorbance maximum increases and the spectrum is shifted towards higher wavelengths as compared to liquid dispersions. The peak characteristic of aggregates does not appear in the spectra of solid phase (2D layer), because the gold particles are unable to get closer to each other. Horovitz et al. also observed that protein was adsorbed on gold surfaces and formed a stable protein layer in all cases [26].

4 Conclusions

Size controlled gold nanoparticles reduced and stabilized by citrate were synthesized. The particles were identified on the basis of their plasmon resonance maxima by UV-Vis spectrometry and their sizes were determined by TEM. The effect of precursor ratio and reducing agent on particle size as well as the size and zeta potential of the aggregates formed were studied by DLS. UV-Vis absorption spectra showed that particles get closer to each other and attach so that the absorbance maxima of spectra shift to the larger wavelengths. The second peak refers to the longitudinal surface plasmon frequencies because of the chain-like attach of gold nanoparticles caused by the cysteine bridge. Values of zeta potential were found to gradually decrease (from -42 to -24 mV) with increasing citrate/gold ratio. The rate of aggregate formation in aquatic gold nanodispersions containing cysteine at various ratios was also studied by DLS. These experiments revealed that large aggregates are not formed in samples containing high amounts of cysteine and due to the stabilizing effect of cysteine the rate constant of aggregation is lower.

Nanorods were synthesized on silanized glass surfaces and particle growth can be followed by AFM. Our experiment shows high concentrations of $HAuCl_4$ deposit thicker gold nanorod layers (~200 nm) on the surface. When cysteine is added to gold sols, their plasmon spectra are shifted due to aggregate forming and by cysteine and glutathione molecules binding to the surface of the gold particles or nanorods.

Acknowledgements

The authors are very thankful for the financial support of the Hungarian Scientific Research Fund (OTKA) Nr. K 73307.

About the authors

Imre Dékány is full professor of chemistry, Head of Department of Colloid Chemistry on University of Szeged. Member of Hungarian Academy of Sciences 2007. Teaching and research interest: colloid and surface chemistry, interfacial phenomena, nanostructured materials. Member of the editorial board: Colloids and Surfaces A, Advances in Colloid and Interface Science, Regional editor of Colloid and Polymer Science.

Andrea Majzik is a Research Fellow at Supramolecular and Nanostructured Materials Research Group of the Hungarian Academy of Sciences. She received her Ph.D. degree in environmental sciences at the University of Szeged this year. Currently her research interests focus on the preparation and characterization of gold and silver nanoparticles and investigations of the interaction between metal nanoparticles and amino acids and protein molecules.

Viktória Hornok is currently a Research Assistant at the Supramolecular and Nanostructured Materials Research Group in the Colloid Chemistry Department. Her research activities focus on the preparation, charachterization and application of Layer-by-Layer thin films (from nanoparticles, polyelectrolytes and proteins). Her research interest includes the near atomic-scale image and thickness determination of thin films by Atomic Force Microscope.

Rita Patakfalvi graduated in chemistry at the University of Attila József, Szeged, Hungary and started to work in the Nanostructured Research Group of the Hungarian Academy of Sciences. She received her Ph.D. degree in environmental sciences at the University of Szeged, Hungary in 2004. Her main research interest is the preparation and characterization of noble metal nanoparticles. Currently she is research scientist at “Centro Universitario de los Lagos”, at the University of Guadalajara, Mexico.

References

1 H. Bonnemann, R.M. Richards, *Inorg. Chem*, 2001, **10**, 2455
2 J. Turkevich, *Gold Bulletin*, 1985, **18**, 3
3 Y. Shao, Y. Jin, S. Dong, *Chem. Commun*, 2004, **9**, 1104
4 Y.Q. He, S.P. Liu, L. Kong, Z.F. Liu, *Spectrochimica Acta Part A*, 2005, **61**, 2861
5 S.M. Saraiva and J.F. de Oliveira, *J. of Dispersion Science and Technology*, 2002, **23**, 6, 837
6 Y. Luo, *Materials Letters*, 2007, **61**, 11-12, 2164
7 Y. Lou, *Materials Letters*, 2007, **61**, 4-5, 1039
8 Y. Luo, *J. of Nanoscience and Nanotechnology*, 2007, **7**, 2, 708
9 H. Chen, Y. Wang, Y. Wang, S. Dong, E. Wang, *Polymer*, 2006, **47**, 763
10 D. Andreescu, T. Kumar Sau, D.V. Goia, *J. Colloid and Int. Science*, 2006, **298**, 742
11 J. Pérez-Juste, I. Pastoriza-Santos, L.M. Liz-marzán, P. Mulvaney, *Coordination Chem. Rev*. 2005, **249**, 1870
12 L.M. Liz-Marzán, *J. Mater. Chem*, 2006, **16**, 3891
13 L.M. Liz-Marzán, *Materials today*, 2004, 26
14 P. Mulvaney, J. Pérez-Juste, M. Giersig, L.M. Liz-Marzán, C. Pecharromán, *Plasmonics*, 2006, **1**, 61
15 R.M. Bright, D.G. Walter, M.D. Musick et al, *Langmuir*, 1996, **12**, 810
16 R. Elghanian, J.J. Storhoff, R.C. Mucic, R.L. Letsinger, C.A. Mirkin, *Science*, 1997, **277**, 1078
17 R. Elghanian, J.J. Storhoff, R.C. Mucic, R.L. Letsinger, C.A. Mirkin, *Langmuir*, 1996, **12**, 810
18 Z. Zhong, S. Patskovsky, P. Bouvrette, H.T. Luong, A. Gedanken, *J. Phys Chem. B*, 2004, **108**, 4046
19 K.H. Lee, K.M. Huang, W.L. Tseng, T.C. Chiu, Y.W. Lin and H.T. Chang, *Langmuir*, 2007, **23**, 1435
20 Z. Wei and F.P. Zamborini, *Langmuir*, 2004, **20**, 11301
21 N.R. Jana, L. Gearheart, C.J. Murphy, *Langmuir*, 2001, **17**, 6782
22 S.H. Brewer, W.R. Glomm, M.C. Johnson, M.K. Knag, S. Franzen, *Langmuir*, 2005, **21**, 9303
23 T. Jensen, L. Kelly, A. Lazarides, G.C. Schatz, *J. of Cluster Science*, 1999, **10**, 2, 295
24 Z. Ma, H. Han, *Coll. And Surf. A*, 2008, **317**, 229
25 O. Horovitz, G. Tomoaia, A. Mocanu, T. Yupsanis, M. Tomoaia-Cotisel, *Gold Bulletin*, 2007, **40/3**, 213
26 O. Horovitz, G. Tomoaia, A. Mocanu, T. Yupsanis, M. Tomoaia-Cotisel, *Gold Bulletin*, 2007, **40/4**, 295